Journal of Sound and Vibration 557 (2023) 117750

Contents lists available at ScienceDirect

Journal of Sound and Vibration

journal homepage: www.elsevier.com/locate/jsvi

A frequency-domain approach to model vertical crowd-structure interaction in lightweight footbridges

Christian Gallegos-Calderón [a,*], Javier Naranjo-Pérez [a,b], Carlos M.C. Renedo [a], Iván M. Díaz [a]

[a] E.T.S.I. Caminos, Canales y Puertos, Universidad Politécnica de Madrid, Calle del Profesor Aranguren 3, 28040, Madrid, Spain
[b] E.T.S. Ingeniería, Universidad de Sevilla, Camino de los Descubrimientos s/n, 41092, Seville, Spain

ARTICLE INFO

Keywords:
Human-structure interaction
Crowd-structure system
Lightweight footbridges
FRP pedestrian structure
Frequency domain

ABSTRACT

Load models that account for Human-Structure Interaction (HSI) may be preferable to accurately predict the dynamic response of lightweight footbridges subjected to pedestrian actions. Representing each person within a crowd may not be practical in engineering design calculations as time-variant models with a large number of degrees of freedom have to be managed. In addition, high computational time may be required to achieve the steady-state response. In this sense, this paper proposes a novel approach to calculate the vertical steady-state response of footbridges from a time-invariant coupled crowd-structure system. Considering the model of the structure and a feedback model of the crowd, a total closed-loop Transfer Function (TF) of the coupled system is derived. Based on this frequency-domain interacting methodology, a step-by-step procedure is set to asses the vibration serviceability of lightweight footbridges due to harmonic excitations through simple algebraic operations. The proposal is used to study a Fibre Reinforced Polymer footbridge subjected to two streams of walking pedestrians. For this structure, a good compromise between experimental and numerical results is obtained in terms of vertical vibrations and TFs. To further validate the proposed approach, a pre-stressed concrete laboratory facility is also analysed, obtaining a satisfactory agreement between the experimental and numerical TFs. Thus, the proposed approach allows to evaluate lightweight footbridges under crowd-induced loads considering HSI in a simple and accurate manner, which is clearly geared to practice.

1. Introduction

In recent years, the adoption of innovative construction techniques and novel materials has led to slender and lightweight pedestrian structures [1–3]. Thus, a lively dynamic response may be expected in these footbridges when subjected to human actions. To assess a lightweight bridge at Vibration Serviceability Limit State (VSLS), guidelines, such as *SETRA* [4] or *HIVOSS* [5], presented pedestrian load models based on experimental and numerical studies carried out in the first years of the current century. Since these models represent the pedestrians as external forces, neglecting the influence of the human body on the dynamic behaviour of the footbridge, they can be classified as non-interacting load models. The new proposals for Eurocodes [6,7] have incorporated the load models from the mentioned design guidances to evaluate the dynamic performance of footbridges. Additionally, modern experimental measurement techniques [8–10] are available to better characterize the forces exerted by people on lightweight pedestrian structures.

* Corresponding author.
E-mail address: christian.gallegos@upm.es (C. Gallegos-Calderón).

https://doi.org/10.1016/j.jsv.2023.117750
Received 17 October 2022; Received in revised form 17 April 2023; Accepted 24 April 2023
Available online 28 April 2023

An issue related to the pedestrian load models available in existing guidelines [4,5] is that only low harmonics of human actions are considered to compute the response of a lightweight bridge. For walking, this assumption is based on the concept that a structure can be significantly excited in the vertical direction just with the first or second harmonic of the human action. Nevertheless, higher harmonics have been found to contribute considerably to the structural acceleration of lightweight pedestrian structures [11,12]. Another issue of applying non-interacting load models when assessing the response of lightweight footbridges is the large differences between the experimental and numerical vibration levels. The main reason for the discrepancies is due to the omission of Human-Structure Interaction (HSI) phenomenon [13,14]. If vibration response of a footbridge could be predicted adequately by accounting for HSI, over-dimensioning structural elements could be avoided. In addition, the inertial mass of a vibration control device for a pedestrian structure may be reduced when the interaction phenomenon is considered [15].

Among the different proposals to account for HSI in the vertical direction [16–19], Single-Degree-of-Freedom (SDOF) systems, defined by the parameters of the human body, acting on the structure have been employed to represent a pedestrian. To model the effects of a continuous stream of pedestrians walking on a footbridge, while considering HSI, several moving SDOF systems to represent the individuals in a crowd have been used [20]. For instance, a SDOF Mass–Spring–Damper (MSD) system plus an external harmonic force have been used to describe active people [21–23]. A SDOF Mass–Spring–Damper–Actuator (MSDA) system has also been employed to represent humans exciting a structure [24,25]. The aforementioned systems, which may be classified as interacting models, are equivalent and lead to the same results when computing the response of a lightweight footbridge under the action of a single walking person [26]. One of the drawbacks of using interacting load models is the high computational time required to achieve a steady-state response when the bridge is analysed under the action of a stream of pedestrians.

Another approach to indirectly account for HSI while still using non-interacting load models recommended in design guidelines is the modification of the modal parameters of the bare structure due to the pedestrians. In Ahmadi et al. [27], an empirical expression is given to calculate the contribution of the pedestrians to the damping of a simply supported structure. Recently, a simplified procedure to consider vertical interaction between a crowd and a footbridge has been proposed by Van Nimmen et al. [28]. Charts in terms of the pedestrian-to-structure mass ratio (up to 0.30) and the modal parameters of the empty structure are employed in this methodology to define an equivalent SDOF system with an effective natural frequency and a damping ratio. As low-frequency structures (<6 Hz) were considered, the proposed charts may not be applicable to very lightweight footbridges, where higher harmonics of pedestrians actions may excite the structure significantly. Furthermore, pedestrian-to-structure mass ratios can be surpassed in structures comprised of novel materials, such as Fibre Reinforced Polymers (FRPs) or aluminium alloys.

Even though non-interacting and interacting load models are usually employed in time-domain analyses, frequency-domain methods are preferable and more useful for assessing the response of a footbridge due to a continuous harmonic excitation. Thus, a general approach, based on the closed-loop Transfer Function (TF) of a coupled crowd-structure system is proposed to predict the steady-state response of a structure subjected to a continuous pedestrian stream. The fundamental vibration mode of the structure, represented as a SDOF MSD system, and the crowd, depicted as a distributed MSDA system, are used in this frequency-domain methodology. Based on this approach, a simple step-by-step procedure is set to calculate the bridge response due to a walking crowd just through algebraic operations while accounting for HSI.

The proposed procedure is employed to assess a 10-m long FRP footbridge under two crowd scenarios at the VSLS. Weak (0.2 pedestrians/m^2) and dense (0.5 pedestrians/m^2) load cases are considered. Experimental results and numerical predictions, using non-interacting and interacting approaches, are compared in terms of the vertical steady-state response. Additionally, experimental TFs obtained from controlled force tests performed with pedestrians walking on the structure are contrasted with the numerical closed-loop TFs. This comparison is also carried out on a pre-stressed concrete structure to demonstrate that the proposal presents no limitations neither the natural frequency of the structure nor the pedestrian-to-structure mass ratio.

After this introduction, the current pedestrian load models are briefly described in Section 2. The theoretical basis to set the frequency-domain approach together with the VSLS assessment procedure are explained in Section 3. In Section 4, the FRP footbridge is presented, and the experimental response due to streams of walking pedestrians is described. In Section 5, the numerical response of the FRP structure is computed considering non-interacting load models and the proposed interacting approach. In addition, a sensitivity analysis of the parameters of the coupled crowd-structure system is carried out in this section. In Section 6, a comparison between experimental and numerical TFs of the FRP structure is discussed, and a pre-stressed concrete footbridge is also studied employing the proposed approach. Finally, the main conclusions and future steps are presented in Section 7.

2. Current pedestrian load models

The assessment of the dynamic response of a footbridge at VSLS has evolved from considering a single person walking or jogging to scenarios where pedestrian streams that account for different traffic classes (different pedestrian densities) crosses the structure. Current guidelines [4,5] and codes [7] adopt a moving force travelling along the structure to model a single pedestrian. Whilst to consider a stream of pedestrians walking over a footbridge, a distributed harmonic load acting on the bridge deck may be considered (Fig. 1). For this case, CEN [7] suggests to employ the following non-interacting load model to compute the resonant response of a structure

$$q_h(t) = 280\cos\left(2\pi f_{as} t\right) n'\,\psi_w \qquad (\mathrm{N/m^2}) \tag{1}$$

being

$$n' = \frac{10.8\sqrt{\zeta_s\, n}}{S} \qquad \text{for } d < 1 \text{ pedestrian/m}^2 \tag{2}$$

$$n' = \frac{1.85\sqrt{n}}{S} \qquad \text{for } d \geq 1 \text{ pedestrian/m}^2 \tag{3}$$

where f_{as} is the gait frequency assumed to be equal to the footbridge natural frequency under consideration, n' is the number of individuals who walk perfectly synchronized within a crowd of n pedestrians, ψ_w is a reduction coefficient that accounts for the probability that the gait frequency approaches the critical range of natural frequencies under consideration, S is the loaded surface of the footbridge, ζ_s is the damping ratio of the structure and d is the pedestrian density.

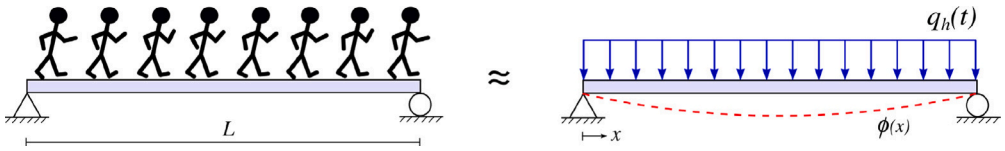

Fig. 1. Non-interacting load model for a stream of walking pedestrians on a footbridge.

The value of 280 in Eq. (1) is obtained by multiplying the static weight of a pedestrian, taken as 700 N, and the Dynamic Load Factor (DLF) that corresponds to the first harmonic of the action ($DFL_1 = 0.40$). The second harmonic of walking action is considered through the reduction of ψ_w from 1 to 0.25. Harmonics higher than 4.8 Hz are not considered in CEN [7]. However, when dealing with very lightweight footbridges, the last consideration may not be applicable since high harmonics of pedestrian actions can contribute to the resonant response. Besides, the interaction phenomenon may be a key factor that affects the dynamic response.

A more sophisticated approach which accounts for HSI is to represent a stream of pedestrians by using as many SDOF systems as individuals within the crowd [14]. In Fig. 2, several MSDA systems moving at a velocity v are displayed as an example. To address the effect that not all pedestrians walk synchronously, a phase shift angle between the human driving forces (F_{ai}) of these SDOF systems should be considered [20]. This type of modelling leads to time-variant coupled dynamic systems, which are computationally expensive and have to be solved by direct numerical integration methods. Additionally, extensive Monte Carlo simulations have to be performed to account for the effect of the variation of pedestrians' properties on the bridge dynamic behaviour [22], and high computational time may be required to achieve the steady-state response. Therefore, representing each person of a crowd may not be practical in engineering design calculations since a problem with a large number of DOFs have to be managed, requiring expertise and advance modelling skills from the users. This approach may not be suitable for future versions of current codes, such as CEN [7].

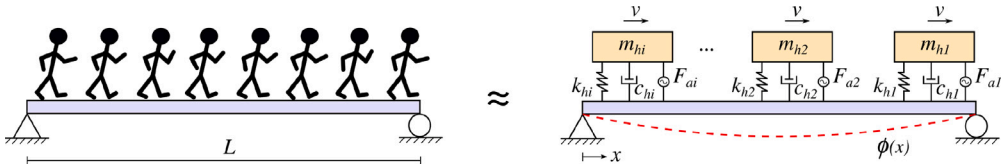

Fig. 2. Representation of a crowd employing several SDOF systems.

To overcome the aforementioned drawbacks, a linear time-invariant (LTI) system may be an alternative. Hence, a general approach in the frequency domain to model Crowd-Structure Interaction (CSI) on lightweight footbridges is proposed hereof. This approach is aligned with current standards, so the steady-state bridge response is computed for a scenario where just few pedestrians within the crowd walk perfectly synchronized. Thus, n' (Eqs. (2)–(3)) is considered for a conservative case of (near-) resonant harmonic excitation.

3. Proposed interacting model

The theoretical basis for the proposed model of the crowd-structure system is presented in this section. Also, a step-by-step procedure is set to estimate accurately and fast the vertical dynamic response of lightweight footbridges subjected to streams of walking pedestrians.

3.1. Crowd-structure system

Considering that n pedestrians are walking freely and unrestricted over the deck of the structure, it can be assumed that all the individuals form a uniformly distributed MSDA system (Fig. 3).

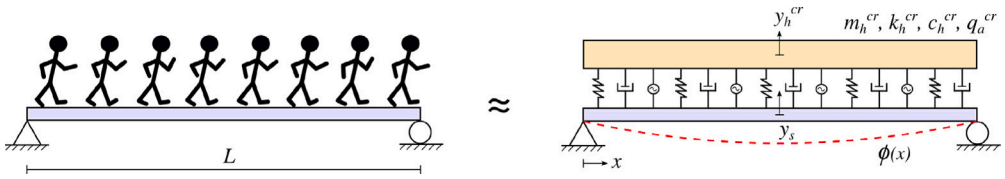

Fig. 3. Representation of a crowd employing a distributed MSDA system.

Based on the dynamic parameters of the human body and the total number of pedestrians (n) acting on the structure, the parameters that define the crowd system (Fig. 3) can be defined as follows

$$m_h^{cr} = \sum_{i=1}^{n} m_{hi} \qquad \text{(kg)} \tag{4}$$

$$c_h^{cr} = \sum_{i=1}^{n} c_{hi} \qquad \text{(Ns/m)} \tag{5}$$

$$k_h^{cr} = \sum_{i=1}^{n} k_{hi} \qquad \text{(N/m)} \tag{6}$$

where m_{hi} (kg) is the mass of the ith pedestrian, $k_{hi} = \omega_{hi}^2 m_{hi}$ (N/m) is the stiffness of the ith human, $\omega_{hi} = 2\pi f_{hi}$ (rad/s) is the ith pedestrian's angular natural frequency, f_{hi} (Hz) is the natural frequency of the ith individual, $c_{hi} = 2\omega_{hi} m_{hi} \zeta_{hi}$ (Ns/m) is the viscous damping of the ith person, and ζ_{hi} is the damping ratio of the ith pedestrian. The superscript 'cr' in the previous and upcoming equations refers to the crowd system. The distributed MSDA system also presents a crowd harmonic driving load associated to the number of pedestrians who walk synchronously (n'), and it may be expressed as follows

$$q_a^{cr}(t) = W_h \, \mathrm{GLF}_r \cos\left(2\pi f_{as} t\right) n' \psi_\omega \qquad \text{(N/m}^2\text{)} \tag{7}$$

where W_h is the weight of a pedestrian and GLF_r is the Generated Load Factor associated to the rth harmonic. Assuming that the gait frequency is always in the critical range of the natural frequencies under consideration, $\psi_\omega = 1$ can be adopted conservatively. Note that the GLF is different from the DLF due to the consideration of HSI. From the distributed load, the crowd driving force (F_a^{cr}) can be computed as follows

$$F_a^{cr}(t) = q_a^{cr}(t)\, S \qquad \text{(N)}. \tag{8}$$

Fig. 4a displays the subsystems, crowd and structure, that comprise the coupled system and the forces that act on them. The crowd driving force per unit length, F_a^{cr}/L (N/m), is assumed to affect both subsystems simultaneously. Similarly, the distributed springs and dampers are considered to generate loads per unit length, F_k^{cr}/L (N/m) and F_c^{cr}/L (N/m) that act on the crowd system and the structure system.

The first equation of motion can be derived from the loads acting on the structure system (bottom part of Fig. 4a) as follows:

$$m_s \ddot{y}_s + c_s \dot{y}_s + k_s y_s = -\int_0^L \frac{F_a^{cr}(t)}{L} \phi(x)\, \mathrm{d}x + \int_0^L \frac{F_c^{cr}(t)}{L} \phi(x)\, \mathrm{d}x + \int_0^L \frac{F_k^{cr}(t)}{L} \phi(x)\, \mathrm{d}x \tag{9}$$

If a sinusoidal form for the unit-normalized fundamental mode shape is assumed

$$\phi(x) = \sin\left(\frac{\pi x}{L}\right) \tag{10}$$

for the case of a simply supported structure, then,

$$\int_0^L \phi(x)\, \mathrm{d}x = \frac{2}{\pi} \tag{11}$$

and Eq. (9) can be rewritten as follows

$$m_s \ddot{y}_s + c_s \dot{y}_s + k_s y_s = \frac{2}{\pi}\left(- F_a^{cr}(t) + F_k^{cr}(t) + F_c^{cr}(t)\right) \tag{12}$$

where y_s (m) is the modal displacement of the structure (upper dots indicating time derivatives), m_s (kg) is the mass associated to a vibration mode of the structure, $c_s = 2\omega_s m_s \zeta_s$ (Ns/m) is the viscous damping of the structure, $\omega_s = 2\pi f_s$ (rad/s) is the structure's angular frequency, f_s (Hz) is the natural frequency, and $k_s = \omega_s^2 m_s$ (N/m) is the stiffness of the structure. At the bottom of Fig. 4b displays the free body diagram of the simply supported structure considering one vibration mode.

Accounting for the crowd harmonic force and the corresponding forces from distributed springs and dampers, a total resulting force on the structure is obtained as follows

$$F_h^{cr}(t) = -F_a^{cr}(t) + F_k^{cr}(t) + F_c^{cr}(t). \tag{13}$$

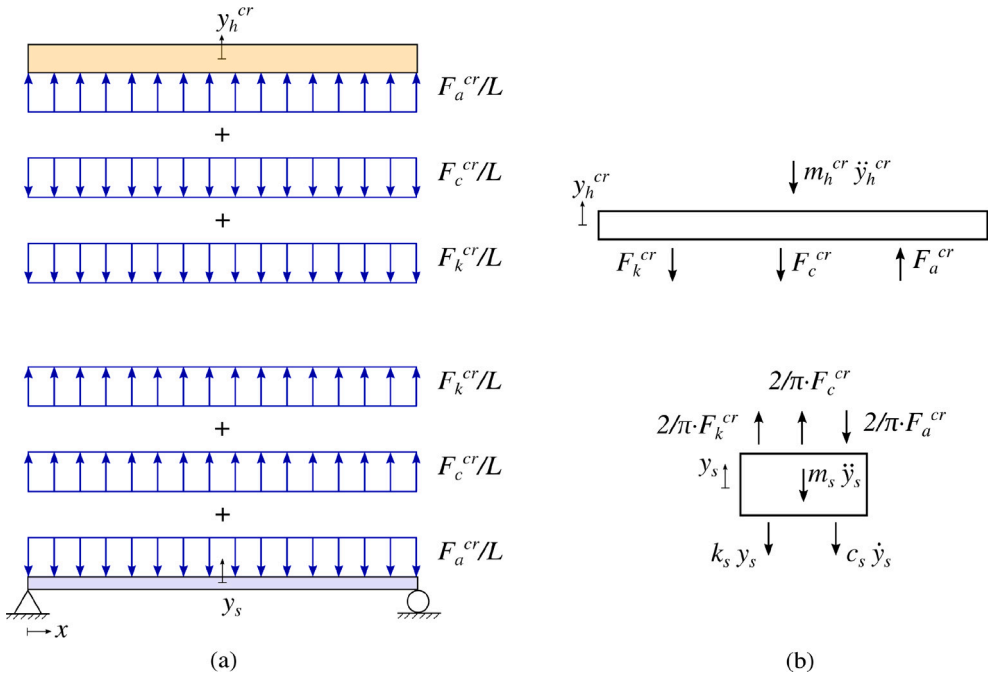

Fig. 4. Coupled crowd-structure system: (a) Forces acting on the crowd system and the structure system, and (b) Free body diagram of the 2 DOFs.

Taking the Laplace transform of Eq. (12), the following expression is derived

$$Y_s(s)\left(m_s\,s^2 + c_s\,s + k_s\right) = 2/\pi\,F_h^{cr}(s) \tag{14}$$

where $s = j\omega$ is the Laplace variable, ω is the angular frequency, $F_h^{cr}(s)$ is the Laplace transform of the resulting force acting on the structure, and $Y_s(s)$ is the Laplace transform of the modal structure displacement.

Multiplying both sides of Eq. (14) by s^2 and rearranging the equation, the TF between the structure acceleration and the resulting force can be obtained as follows

$$s^2Y_s(s) = 2/\pi \cdot \frac{s^2}{m_s\,s^2 + c_s\,s + k_s}\,F_h^{cr}(s) \tag{15}$$

where $s^2Y_s(s)$ is the Laplace transform of the acceleration of the footbridge. The TF of the structure is identified as

$$G_S(s) = \frac{s^2}{m_s\,s^2 + c_s\,s + k_s}. \tag{16}$$

Hence, Eq. (15) can be written as follows

$$s^2Y_s(s) = 2/\pi \cdot G_S(s)\,F_h^{cr}(s). \tag{17}$$

A second equation of motion based on the loads acting on the crowd system (top part of Fig. 4a) can be derived as follows

$$m_h^{cr}\,\ddot{y}_h^{cr} + F_k^{cr}(t) + F_c^{cr}(t) = F_a^{cr}(t) \tag{18}$$

where y_h^{cr} (m) is the displacement of the distributed MSDA system. The free body diagram of the crowd system is presented at the top of Fig. 4b.

Since the footbridge movement influences the crowd motion (and vice versa), it is assumed that the acceleration of the structure affects the distributed MSDA system through the value of $\phi(x)$ along the bridge length. For the case of a simply supported structure, the value is $2/\pi$. This is graphically illustrated in Fig. 5. Thus, the forces associated to the springs and dampers can be expressed as follows

$$F_c^{cr}(t) = c_h^{cr}\left(\dot{y}_h^{cr} - \frac{2}{\pi}\dot{y}_s\right) \tag{19}$$

$$F_k^{cr}(t) = k_h^{cr}\left(y_h^{cr} - \frac{2}{\pi}y_s\right) \tag{20}$$

Accounting for Eqs. (19)–(20) and Eq. (18), the following expression for the crowd system is achieved

$$m_h^{cr}\,\ddot{y}_h^{cr} + c_h^{cr}\left(\dot{y}_h^{cr} - \frac{2}{\pi}\dot{y}_s\right) + k_h^{cr}\left(y_h^{cr} - \frac{2}{\pi}y_s\right) = F_a^{cr}(t). \tag{21}$$

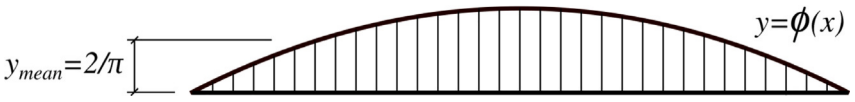

Fig. 5. Mean value of the modal coordinates of $\phi(x)$.

Taking the Laplace transform of Eq. (21) and rearranging the equation, the following expression is derived

$$Y_h^{cr}(s)\left(m_h^{cr}\,s^2 + c_h^{cr}\,s + k_h^{cr}\right) - 2/\pi\, Y_s(s)\left(c_h^{cr}\,s + k_h^{cr}\right) = F_a^{cr}(s) \tag{22}$$

where $Y_h^{cr}(s)$ is the Laplace transform of the displacement of the crowd system, and $F_a^{cr}(s)$ is the Laplace transform of the crowd driving force (Eq. (8)).

Multiplying both sides of Eq. (22) by m_h^{cr} and s^2 and rearranging the equation, the following expression is achieved

$$m_h^{cr}\,s^2 Y_h^{cr}(s) = \frac{m_h^{cr}\,s^2}{m_h^{cr}\,s^2 + c_h^{cr}\,s + k_h^{cr}}\,F_a^{cr}(s) + 2/\pi \cdot \frac{m_h^{cr}(c_h^{cr}\,s + k_h^{cr})}{m_h^{cr}\,s^2 + c_h^{cr}\,s + k_h^{cr}}\,s^2 Y_s(s) \tag{23}$$

where $s^2 Y_h^{cr}(s)$ is the Laplace transform of the acceleration of the distributed MSDA system. From Eq. (23), the TFs associated to the crowd system and the interaction phenomenon are identified, respectively, as follows

$$G_H^{cr}(s) = \frac{m_h^{cr}\,s^2}{m_h^{cr}\,s^2 + c_h^{cr}\,s + k_h^{cr}} \tag{24}$$

$$G_{HSI}^{cr}(s) = \frac{m_h^{cr}(c_h^{cr}\,s + k_h^{cr})}{m_h^{cr}\,s^2 + c_h^{cr}\,s + k_h^{cr}}. \tag{25}$$

Finally, replacing Eq. (13) into Eq. (18) and taking the Laplace transform, the expression presented below is obtained

$$m_h^{cr}\,s^2 Y_h^{cr}(s) = -F_h^{cr}(s) \tag{26}$$

resulting in

$$F_h^{cr}(s) = -G_H^{cr}(s)\,F_a^{cr}(s) - 2/\pi \cdot G_{HSI}^{cr}(s)\,s^2 Y_s(s). \tag{27}$$

Eq. (27) indicates that the resulting force on the structure is the sum of the driving force transmitted through the crowd system (G_H^{cr}) and the interacting force due to the structure response. Based on Eqs. (17) and (27), a block diagram of the crowd-structure system, mainly characterized by a feedback loop associated to HSI, can be assembled as presented in Fig. 6. This diagram employs TFs related to the structure system ($G_S(s)$), crowd system (G_H^{cr}), and interaction phenomenon (G_{HSI}^{cr}).

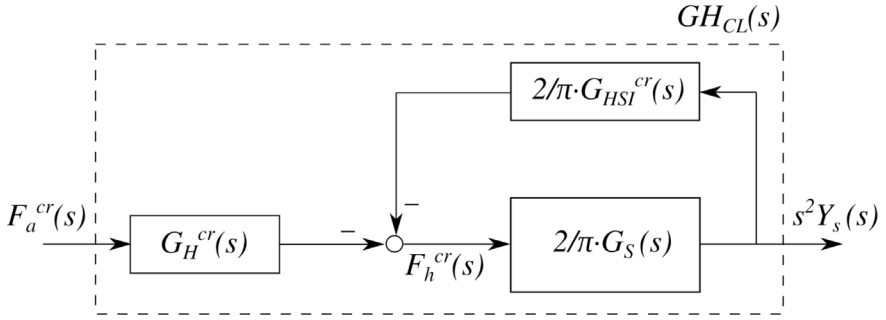

Fig. 6. Block diagram of the crowd-structure system.

From Fig. 6, the 2-DOF system (Y_h^{cr}, Y_s) can be merged in a total closed-loop TF between the acceleration of the structure ($s^2 Y_s(s)$) and the crowd driving force ($F_a^{cr}(s)$). This TF is derived through algebraic operations with the blocks, resulting in the following expression

$$GH_{CL}(s) = \frac{s^2 Y_s(s)}{F_a^{cr}(s)} = \frac{(2/\pi)\cdot G_S(s)\,G_H^{cr}(s)}{1 + (2/\pi)^2 \cdot G_S(s)\,G_{HSI}^{cr}(s)} \qquad \text{with } s = j\omega. \tag{28}$$

To compute the steady-state acceleration response of the structure, Eqs. (7)–(8) and the closed-loop TF from Eq. (28) are employed. Thus, the following expression can be used

$$\ddot{y}_s(t) = \left|GH_{CL}(j\omega)\right|_{\omega=2\pi f_{as}} \cdot \left(W_h\,\mathrm{GLF}_r\,n'\,\psi_\omega\,S\right)\cos\left(2\pi f_{as} t\right). \tag{29}$$

The maximum response due to the resonant harmonic of the pedestrian action may be further simplified through an algebraic multiplication, using the following expression

$$\mathrm{a}_{\mathrm{peak}} = \max_{j\omega} \left| GH_{CL}(j\omega) \right| \cdot \left(W_h \, \mathrm{GLF}_r \, n' \, \psi_\omega \, S \right) \tag{30}$$

where the maximum value of $\left| GH_{CL}^{eq}(j\omega) \right|$ is the H_∞ norm of the total closed-loop TF presented in Eq. (28).

Given this approach considers the resonant response of the bridge, the Maximum Transient Vibration Value (MTVV) may be employed for the assessment of a footbridge at VSLS, as suggested by ISO [29]. The MTVV can be calculated as

$$\mathrm{MTVV} = \frac{\mathrm{a}_{\mathrm{peak}}}{\sqrt{2}}. \tag{31}$$

3.2. Step-by-step procedure

Considering the explanation in Section 3.1 and summarizing, the following steps may be used to predict the dynamic response of a footbridge while considering CSI:

1. Define the parameters of the considered vibration mode of the structure (m_s, f_s, and ζ_s).
2. Set the number of pedestrians walking on the structure (n).
3. Define the parameters of the human body (m_h, f_h, and ζ_h).
4. Determine the parameters of the crowd system (m_h^{cr}, f_h^{cr}, and ζ_h^{cr}) through Eqs. (4)–(6).
5. Obtain the total closed-loop TF of the crowd-structure system ($GH_{CL}(j\omega)$) using Eq. (28).
6. Compute $\mathrm{a}_{\mathrm{peak}}$ employing Eq. (30) for evaluating the structure at VSLS.

Note that if a comparison between measurements and numerical results is required, the maximum value calculated from the experimental 1s-running Root-Mean-Square acceleration may also be employed. Hence, MTVVs obtained from a test and a simulation can be contrasted.

4. FRP footbridge and experimental tests

This section presents the FRP footbridge which is later employed to apply the proposed frequency-domain procedure. Additionally, the acceleration response of the bridge due to the action of walking pedestrians is presented.

4.1. Description of the structure

The footbridge is a simply supported structure of 10.0 m long by 1.5 m wide, as displayed in Fig. 7a. Pultruded Glass-FRP (GFRP) elements and Carbon-FRP (CFRP) strips, manufactured by Fiberline Composites A/S [30], are employed to assemble the bridge. GFRP panels (Plank HD) placed onto three GFRP stringers (1 I 300 × 150 × 15 and 2 U 300 × 90 × 15) comprise the superstructure. Additionally, GFRP crossbeams (I 160 × 80 × 8) restrained laterally the stringers, and CFRP strips (1 E 139/150/4.9 and 2 E 139/90/4.9) are adhesively bonded to the flanges of the stringers along their length. For the handrails, GFRP profiles (SHS 60 × 60 × 5) and stainless-steel cables are used. The connections among the aforementioned GFRP elements are achieved employing stainless-steel bolts class A2-50 and GFRP profiles (L 75 × 75 × 8). At the bridge ends, concrete blocks are placed for the installation of pinned and roller supports (Fig. 7a). A detailed description of the structural design of the FRP footbridge, whose linear mass is about 80 kg/m, can be found in Gallegos-Calderón et al. [31].

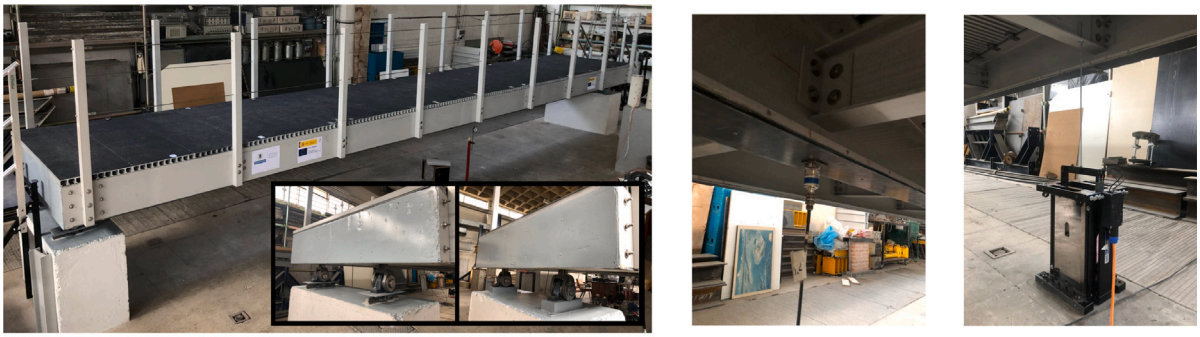

(a) (b) (c)

Fig. 7. FRP footbridge: (a) Built structure, (b) Accelerometer at midspan, and (c) Shaker in a fixed body mode.

Prior the tests involving pedestrians, an Operational Modal Analysis (OMA) was performed to identify the vibration modes of the structure [26]. The first vibration mode of the FRP bridge (Fig. 8a) is a bending vertical mode at 7.66 Hz, whereas the second

and third vibration modes are lateral torsional modes at 10.96 and 15.01 Hz, respectively. Then, controlled force experiments concentrated on the first vibration mode of the structure were carried. The acceleration collected from a piezoelectric sensor model 393A03 (sensitivity 1 V/g and 0.00001 g RMS wide band resolution) [32] attached at the bottom of the central stringer (Fig. 7b) and a controlled force applied from an electrodynamic shaker APS 400 [33] (Fig. 7c) were used to obtain experimentally the TF between both magnitudes. Since the electrodynamic device was set-up in a fixed body mode, the force generated by the device was obtained by monitoring its instantaneous current during the tests. A stainless-steel rod connected the shaker to a crossbeam near the edge of the midspan cross-section. The input signal to the shaker was a chirp waveform whose instantaneous frequency increases slowly and linearly from 6 to 9 Hz during 5 min, ensuring that the sweeping at each frequency was sufficiently slow to obtain a satisfactory identification of the TF of the first vertical vibration mode of the bridge.

Three tests considering the bare footbridge were conducted varying the shaker force level and the corresponding TFs were computed through the H_1 estimator. Thus, a representative (mean) TF was obtained, as shown in Fig. 8b. In this graph, the width of the coloured band corresponds to the minimum and maximum values among the three identified TFs. A reasonable linear behaviour can be seen. From the mean TF, a natural frequency (f_s) of 7.47 Hz, a damping ratio (ζ_s) of 1.40%, and an effective modal mass (m_s) of 405 kg are identified. The difference between the value of the fundamental frequency from the OMA and the experimental modal analysis is explained by the activation, or not, of the roller support. The FRP footbridge appears to be slightly stiffer when negligible excitation (OMA test) is applied.

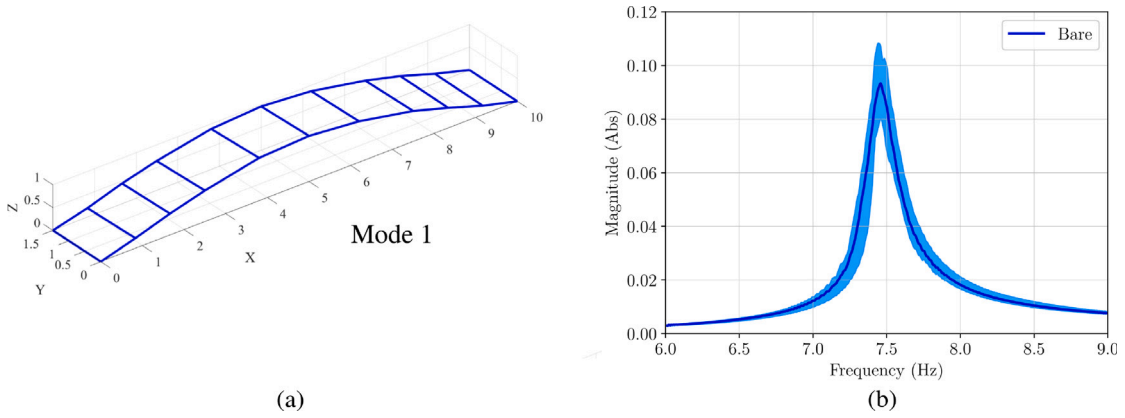

Fig. 8. Experimental characterization of the first vibration mode of the bare FRP footbridge: (a) Mode shape from the OMA, and (b) TF.

4.2. Dynamic response assessment

The dynamic response of the FRP footbridge under the action of two crowd scenarios is presented herein. For the tests, the piezoelectric accelerometer shown in Fig. 7b was employed to collect the response of the bridge at midspan. Fig. 9 displays the experiments carried out. Three and eight people walking continuously for 5 min over the deck were considered to represent weak and dense Traffic Classes (TCs), respectively. The duration of each test was also selected to obtain a representative value of the steady-state response of the footbridge. In Table 1, the total mass of the people involved in each test and the pedestrian-to-structure mass ratio, accounting for the mass of the FRP footbridge, are presented.

Table 1
Mass of the pedestrians involved in the experiments.

Traffic class	Number of pedestrians	d (pedestrians/m^2)	Total mass of pedestrians (kg)	Mass ratio
Weak	3	0.20	218.8	0.27
Dense	8	0.53	585.7	0.73

First, the weak TC was analysed, so three pedestrians were asked to walk comfortably and freely along the full length of the bridge (Fig. 9a). Neither the distance among individuals nor the gait frequency were set during the test, and overtaking was allowed. The response was recorded with a sampling frequency of 1000 Hz using the sensor shown in Fig. 7b. The measured raw data is shown in Fig. 10a, where the maximum acceleration is 4.82 m/s^2 and the MTVV is 1.23 m/s^2. Then, the signal was processed using a zero-phase 4th order band-pass Butterworth filter with an upper and lower cut-off frequencies at 1 Hz and 20 Hz, respectively. The resulting signal is displayed in Fig. 10b, where the peak response is 2.14 m/s^2 and the MTVV is 1.22 m/s^2. As expected, the maximum acceleration decreases significantly since values associated to high-frequency components are disregarded once the filter is applied. Nevertheless, the computed MTVVs remain almost identical. Hence, this parameter is assumed to be a representative and robust value for the VSLS assessment.

Fig. 9. Experiments carried out considering: (a) weak TC, and (b) dense TC.

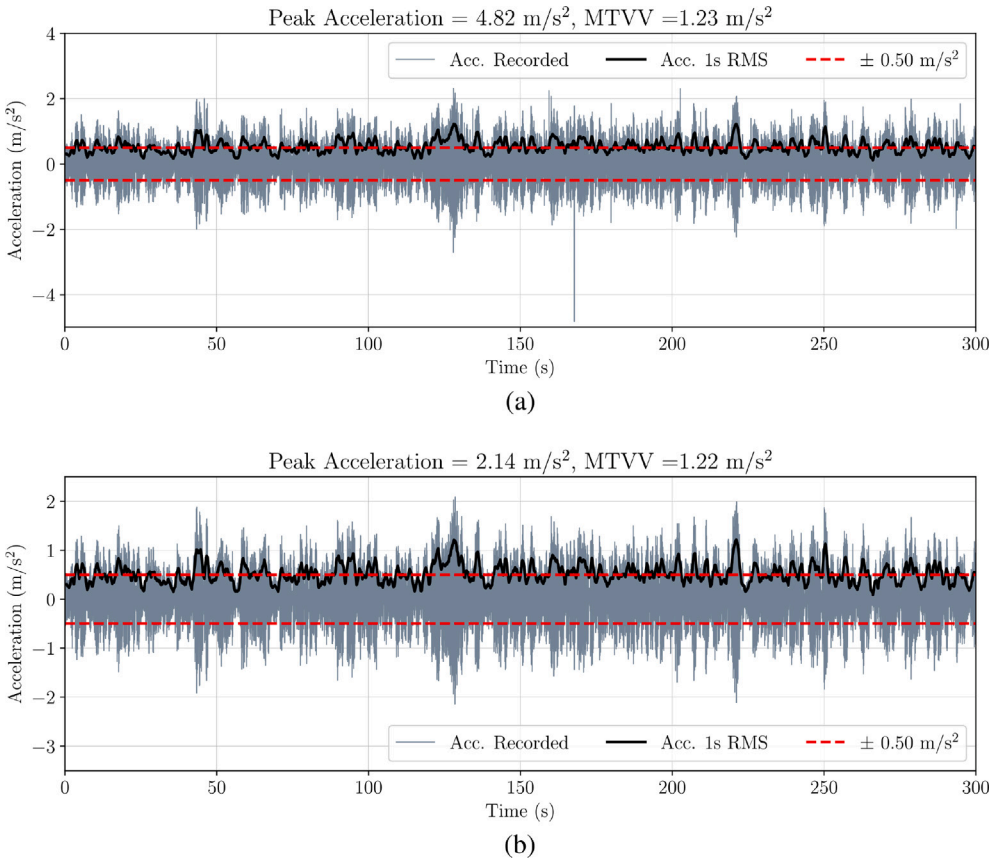

Fig. 10. Response of the FRP footbridge due to a weak TC: (a) Raw data, and (b) Processed signal with a zero-phase 4th order band-pass Butterworth filter between 1 and 20 Hz.

Second, the dense TC was studied. Eight pedestrians walked in the same manner as previously explained (Fig. 9b). The recorded data was processed employing the same zero-phase 4th order band-pass Butterworth filter. Fig. 11 displays the response, where the maximum acceleration is 2.42 m/s^2 and the MTVV is 1.20 m/s^2. In comparison with the weak TC, the peak response increased 13% whilst the MTVV slightly decreased 2%.

To determine the harmonic (r) of the walking action that is mainly exciting the structure, the Fast Fourier Transform of the processed signals were computed. In Fig. 12, the spectrum of the footbridge response is presented for the two crowd scenarios. Considering the peaks in the graphs, it is appreciated that the structural acceleration is mainly associated to the fourth harmonic.

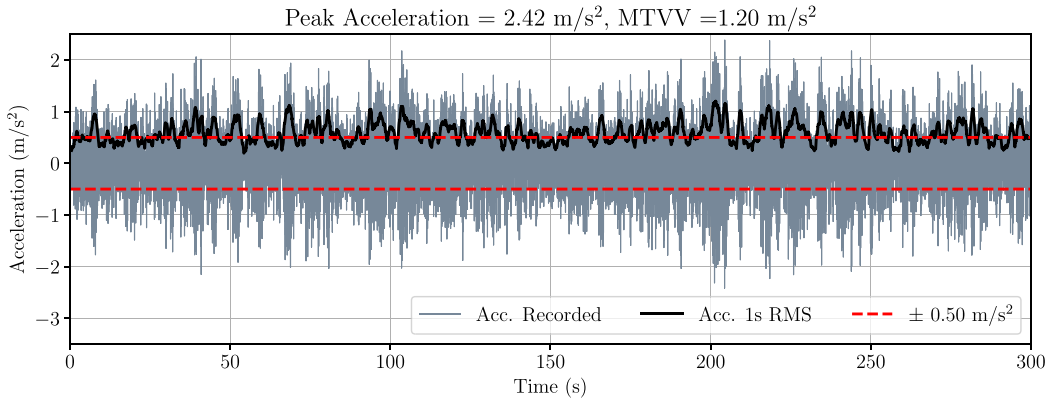

Fig. 11. Response of the FRP footbridge due to a dense TC using a zero-phase 4th order band-pass Butterworth filter between 1 and 20 Hz.

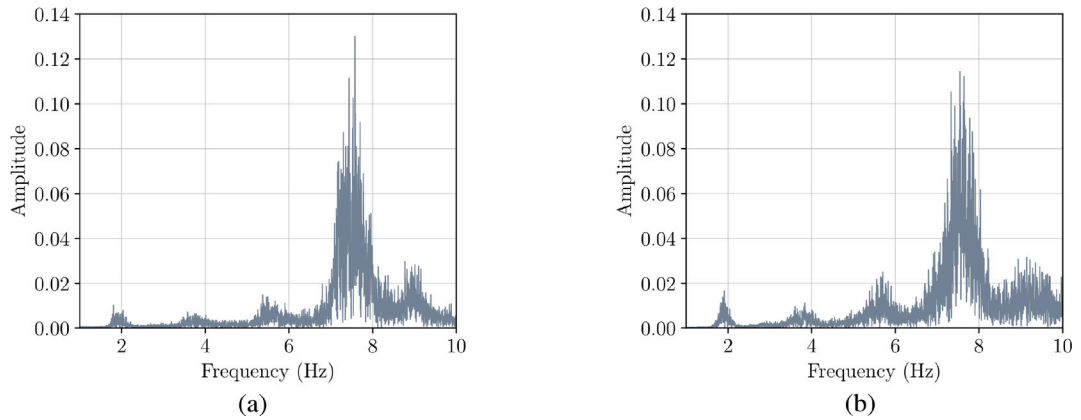

Fig. 12. Spectrum of the response: (a) Weak TC, and (b) Dense TC.

5. Application of the proposed approach

Considering the experimental results obtained previously, the proposed frequency-domain approach is applied in this section. For the sake of comparison, the non-interacting load models recommended by CEN [7] are firstly employed to calculate response of the FRP footbridge for the two TCs. Then, the vibration levels of the structure are assessed following the step-by-step procedure described in Section 3.2. A sensitivity analysis considering uncertainties in the systems of the structure and the crowd is also presented using the proposed procedure.

5.1. Non-interacting approach

A Finite Element (FE) model developed in ABAQUS [34] is employed to predict the response of the FRP structure. Fig. 13a displays the model, where node reduced integration shell elements (S4R) are used to represent the stringers, cross-beams, handrail poles, and deck. The concrete blocks are defined with solid elements C3D8R. To model the GFRP laminate and the CFRP strip in each flange of the stringers, shell composite layups composed of two plies are employed. The stringers, cross-beams, and handrail poles are connected through the tie constraint option. To join together the stringers' top flange and the bottom part of the deck, connector elements type CONN3D2 every 25 mm along the stringers' length are modelled. Also, the stringers are connected to the concrete blocks using the embedded element technique. The size of the mesh for all the elements is 30 mm × 30 mm. For the boundary conditions, displacements of two areas of 0.20 m by 0.15 m at the bottom of one concrete block are constrained in x, y and z directions. At the bottom of the other block, the displacements in the y and z directions of two similar areas are constrained. Given that L profiles, washers, nuts and bolts are omitted in the model, 2.0 kg/m^2 over the deck is assumed as an additional non-structural mass.

Employing the FE model, whose numerical calibration is described in Gallegos-Calderón et al. [26], the response of the structure considering the first vertical vibration mode (Fig. 13b) is assessed. For the two crowd scenarios, the non-interacting load acting on the FRP footbridge is obtained from Eq. (1) and the total mass of the pedestrians (Table 1) is assumed to be uniformly distributed over the bridge deck as additional non-structural mass.

For the weak TC, the parameters to obtain $q_h(t)$ (Eq. (1)) are: $n = 3$ pedestrians, $\zeta_s = 1.40\%$ and $S = 15$ m^2. The fundamental frequency of the FE model decreases due to the pedestrian mass (14.60 kg/m^2), so $f_{as} = 6.78$ Hz is set to calculate a resonant response. Also, $\psi_\omega = 0.15$ is assumed since the FRP structure is excited by the fourth harmonic of walking action. This value is derived from the $DLF_4 = 0.06$ [29] and the pedestrian static weight. Therefore, $280 \cdot \psi_\omega$ is equal to $700 \cdot DLF_4$ in order to consider the fourth harmonic. The numerical response of the FRP structure for this case is presented in Fig. 13c, where the peak acceleration is 3.77 m/s^2 and the MTVV is 2.69 m/s^2.

For the dense TC, the parameters to compute $q_h(t)$ are: $n = 8$ pedestrians, $\zeta_s = 1.40\%$, $S = 15$ m^2, $f_{as} = 5.84$ Hz considering a pedestrian mass of 39.05 kg/m^2, and $\psi_\omega = 0.15$. The acceleration computed for this crowd scenario is displayed in Fig. 13d, where the maximum response is 4.55 m/s^2 and the MTVV is 3.24 m/s^2. In the two analysed cases, it is clear that the non-interacting load models lead to a poor prediction (significant over estimation) of the vibration levels on the FRP footbridge, as compared with Figs. 10b and 11.

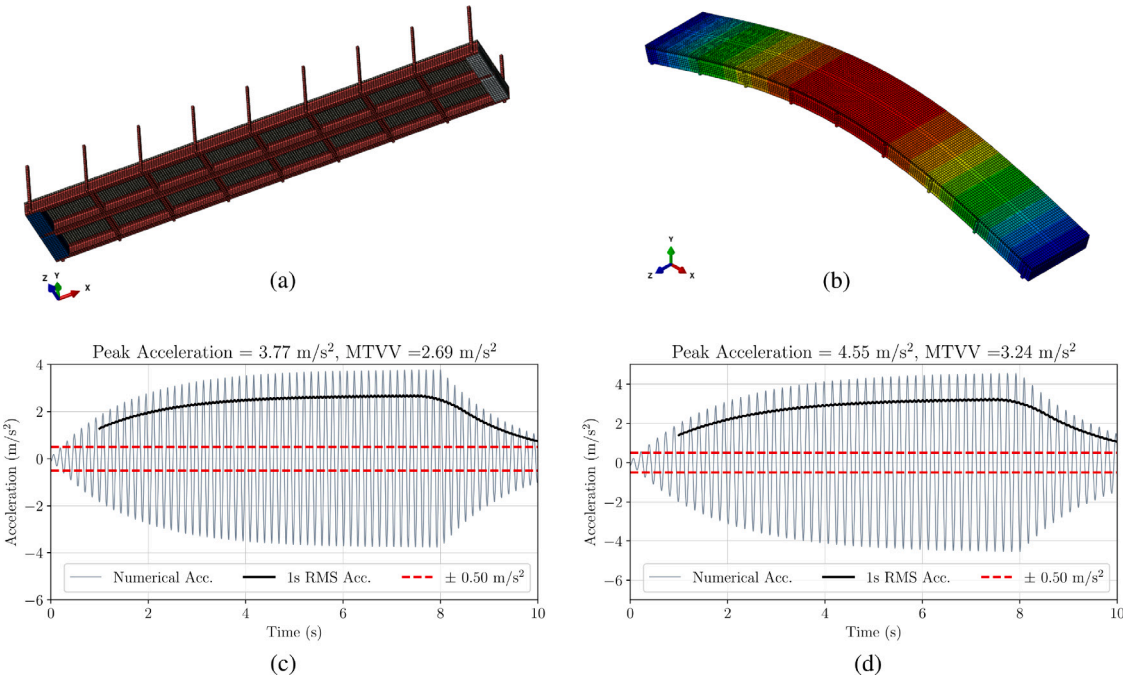

Fig. 13. Non-interacting approach: (a) FE model, (b) First vertical vibration mode, (c) Response due to a weak TC, and (d) Response due to a dense TC.

5.2. Interacting approach

Adopting the proposed frequency-domain approach, the response of the lightweight structure is assessed under the same actions of weak and dense TCs. Following the steps in Section 3.2, the results are:

1. Parameters of the vibration mode of the structure: $m_s = 405$ kg, $f_s = 7.47$ Hz, and $\zeta_s = 1.40\%$.
2. Number of pedestrians walking on the structure: $n = 3$ for the weak TC, and $n = 8$ for the dense TC.
3. Parameters of the human body: $m_h = 0.93 \cdot 72.90$ kg for the weak TC, $m_h = 0.93 \cdot 73.20$ kg for the dense TC, $f_h = 1.88$ Hz and $\zeta_h = 23.40\%$ [26]. The values of 72.90 kg and 73.20 kg are obtained from the average mass value of the pedestrians involved in the experiments (Table 1).
4. Parameters of the crowd system: Table 2 presents the values for each TC.
5. Closed-loop TF of the crowd-structure system: Fig. 14 displays the amplitude of the total TFs obtained for both crowd scenarios.
6. Computation of the response: $W_h = 700$ N, $GLF_4 = 0.037$ [26], and $S = 15$ m^2. Table 3 presents the results of $n' \cdot S$ (number of pedestrians walking synchronously on the bridge), F_a^{eq} (computed according to the value of n'), the H_∞ norm (maximum value of $|GH_{CL}(j\omega)|$), a_{peak}, and MTVV for each crowd scenario.

It can be seen that the MTVVs obtained experimentally (Figs. 10–11) and those obtained by the proposed procedure (Table 3) are similar for both crowd scenarios. This demonstrates that the dynamic response prediction may be easily carried out using the proposed simplified approach.

Table 2
Parameters of the crowd system for each TC.

Parameter	Weak TC	Dense TC
m_h^{cr} (kg)	203.5	544.7
k_h^{cr} (N/m)	2.84×10^4	7.60×10^4
c_h^{cr} (N s/m)	1.12×10^3	3.01×10^3

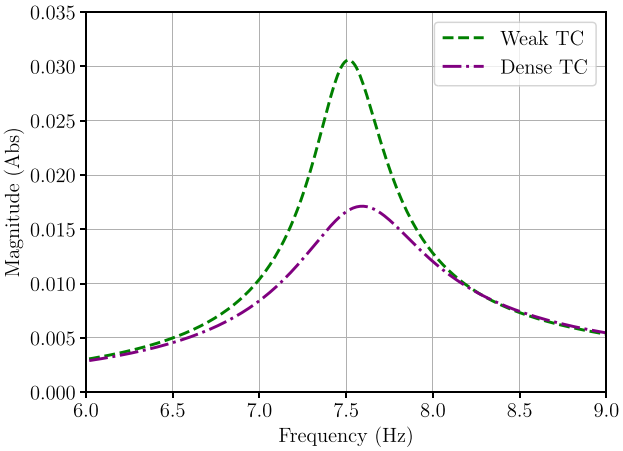

Fig. 14. Closed-loop TFs, $\left|GH_{CL}^{eq}(j\omega)\right|$.

Table 3
Results following the proposed approach.

Parameter	Weak TC	Dense TC
$n' \cdot S$ (pedestrians)	2.21	3.61
F_a^{cr} (N)	55.55	91.05
H_∞ norm (m/s^2/N)	0.0306	0.0171
a_{peak} (m/s^2)	1.70	1.56
MTVV (m/s^2)	1.20	1.10

Table 4 presents the MTVVs obtained in the experiments and through the different approaches for the two studied load cases. Regarding the peak values, significant differences between numerical results and measurements (2.14 m/s^2 for the weak TC, and 2.42 m/s^2 for the dense TC) are obtained. This is explained by the definition of the load in Eq. (7), which only accounts for the resonant harmonic of the pedestrian action. Whilst in the experimental results (Figs. 10b and 11), the contribution of the other harmonics are also considered due to the band-pass filter between 1 and 20 Hz employed.

Table 4
MTVVs (m/s^2).

Traffic scenario	Experimental	Non-inter. approach	Error (%)	Proposed approach	Error (%)
Weak	1.22	2.69	+120	1.20	−2
Dense	1.20	3.24	+170	1.10	−8

5.3. Sensitivity analysis of the model parameters

To determine the influence of the model parameters of the crowd system and structure system in the proposed approach, a sensitivity analysis is carried out. The vibration mode of the FRP footbridge and the distributed MSDA system are defined through statistical distributions. A normal distribution ($\mathcal{N}(\mu, \sigma)$) is assumed for m_s. Similarly to stiffness and strength properties of pultruded FRP elements [35], a two-parameter Weibull distribution ($\mathcal{W}(\mu, \sigma)$) was adopted for f_s and ζ_s. For the parameters of the human body that allow to define the crowd system, a normal distribution is considered for m_h, whilst a uniform distribution ($\mathcal{U}(a, b)$) is assumed for f_h and ζ_h due to the variability of values reported in literature [17]. The definition of the aforementioned parameters are as follows:

- m_s: $\mathcal{N}$(405, 20.30) kg, f_s: $\mathcal{W}$(7.47, 0.37) Hz, and ζ_s: $\mathcal{W}$(1.40, 0.07)%.
- m_h: $\mathcal{N}$(72.90, 3.65) kg, f_h: $\mathcal{U}$(1.50, 3.00) Hz, and ζ_h: $\mathcal{U}$(10, 50)%.

The structural response, in terms of MTVVs, is computed using the proposed frequency-domain approach and accounting for 1000 stochastic samples of each parameter. The results of the analyses are presented in Fig. 15, where the red triangle shows the response calculated using the nominal values for the parameters of FRP footbridge and the human body.

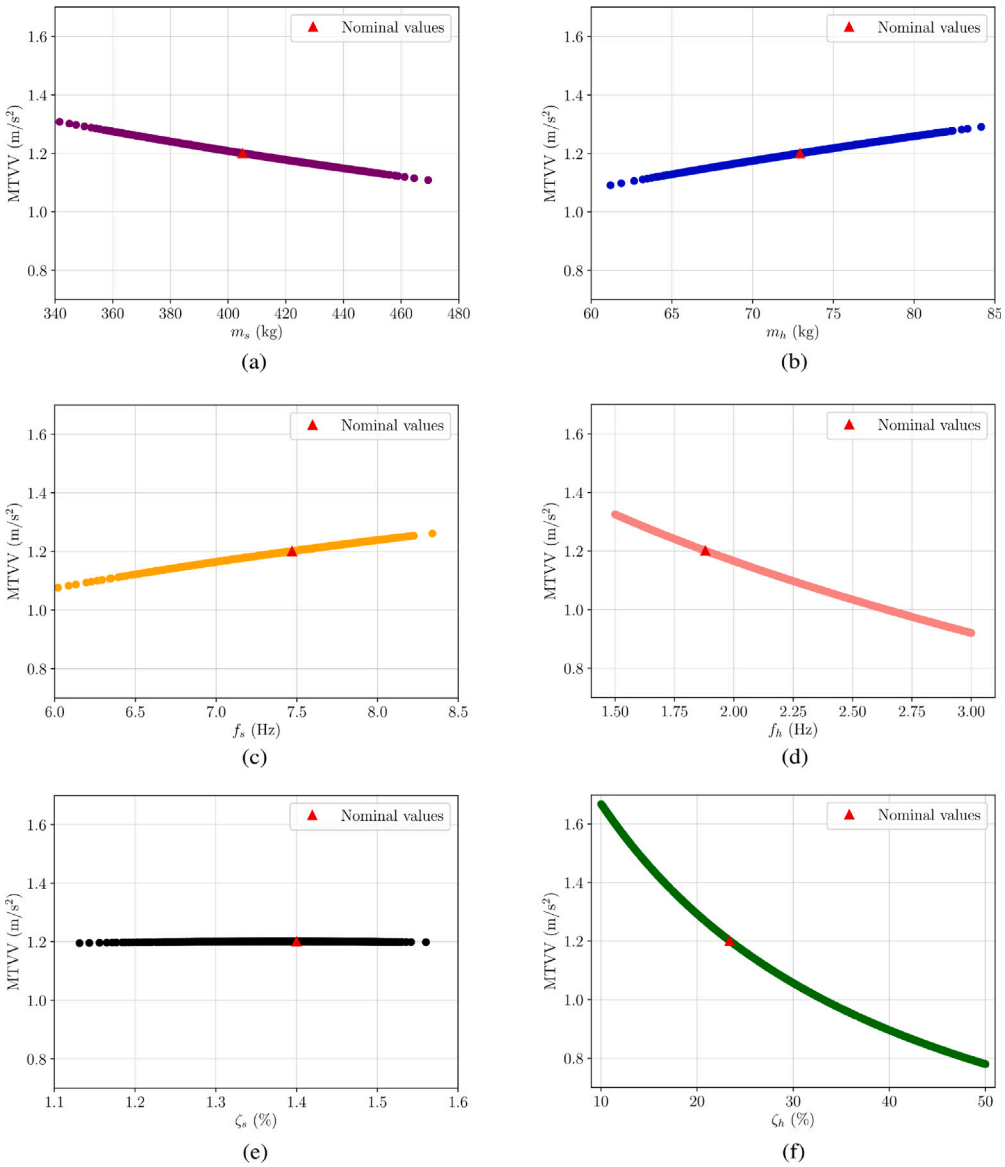

Fig. 15. Sensitivity analysis: (a) m_s, (b) m_h, (c) f_s, (d) f_h, (e) ζ_s, and (f) ζ_h. (For interpretation of the references to colour in this figure legend, the reader is referred to the web version of this article.)

As expected, Fig. 15a shows a reduction of the MTVV as m_s increases, whereas Fig. 15b displays a direct proportional relationship between m_h and the response. In Fig. 15c, it is seen that the increment of f_s does not lead to lower results. As the structure's fundamental frequency moves away from the pedestrian's natural frequency, the influence of the pedestrian on the footbridge response diminishes. On the contrary, increasing f_h leads to a reduction of the vibrations levels, as illustrated in Fig. 15d. Fig. 15e shows that the response is not sensitive to the variation of ζ_s, whilst Fig. 15f demonstrates that the most influential parameter on the results is ζ_h. This is explained by the large difference between the damping ratio of the pedestrian model and the structure, being the first one at least ten times the second one. In general, the parameters associated to the pedestrians, especially ζ_h, seem to be more influential than the parameters of the FRP footbridge on the prediction of the dynamic response.

6. Assessment of HSI in the frequency domain

In this section, HSI is studied in the frequency domain through the comparison of experimental and numerical TFs of the FRP footbridge. A pre-stressed reinforced concrete footbridge, built at Sheffield University and described by Živanović et al. [36], is also

analysed to demonstrate that the proposed approach is general and can be applied independently of the fundamental frequency of the footbridge and the grade of coupling between the crowd and the structure.

In both footbridges, the influence of the damping ratio of the pedestrian (ζ_h) on the closed-loop TF is investigated since it has been identified in the previous section as the most influential parameter in the dynamic response of the coupled system.

6.1. FRP structure

The accelerometer and electrodynamic shaker display in Fig. 7b–c were used to apply controlled forces and identify experimentally the TF of the coupled crowd-structure system with, firstly, three pedestrians walking (Fig. 9a) and, secondly, with eight people walking over the deck (Fig. 9b). Similar to previous investigations [21,36], the test subjects walked freely and comfortably along the full length of the structure. The pedestrians were always on the FRP footbridge during each test since the identification of the TF of the coupled crowd-structure system was aimed. The generated signal as input of the shaker was a chirp waveform, whose instantaneous frequency increases slowly and linearly from 6 to 9 Hz during 5 min. The time was selected to assure that the sweeping at each frequency was sufficiently slow to obtain good quality TFs.

The controlled force test can be represented through the block diagram shown in Fig. 16, in which the pedestrian driving force that affects the structure is filtered by the TF of the crowd system ($F_{ha}^{cr} = F_a^{cr}\, G_H^{cr}(s)$). From this diagram, the structure acceleration can be derived through algebraic operations with the blocks, resulting in the following expression

$$s^2 Y_s(s) = \frac{(2/\pi)\cdot G_S(s)}{1+(2/\pi)^2\cdot G_S(s)\cdot G_{HSI}^{cr}(s)}\, F_{shaker} + \frac{(2/\pi)\cdot G_S(s)}{1+(2/\pi)^2\cdot G_S(s)\cdot G_{HSI}^{cr}(s)}\, F_{ha}^{cr} \tag{32}$$

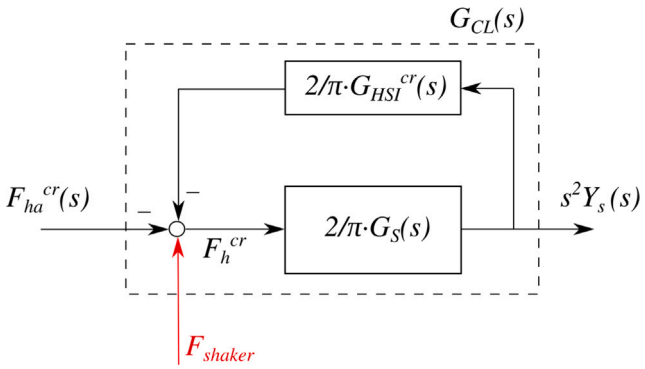

Fig. 16. Block diagram for comparison of TFs.

Considering that the force exerted by the pedestrians is randomly distributed in the frequency range of study and considerably lower than the force generated by the electrodynamic shaker, the second term of Eq. (32) can be neglected. Hence, $G_{CL}(s)$ can be identified experimentally. The previous consideration is based on the idea that the shaker force, whose amplitude measured during the tests was 315 N, is higher than F_{ha}^{cr}, whose amplitude is associated to the fourth harmonic of the walking pedestrians [37]. Therefore, results from the controlled force tests and from Eq. (32) may be comparable. This expression is also valid for the tests involving the bare structure, where $F_{ha}^{cr} = 0$ and $G_{HSI}^{cr}(s) = 0$, so $G_S(s)$ is identified.

For the case of three pedestrians walking on the FRP bridge, TFs calculated from the measurements and the theoretical analysis are contrasted in Fig. 17a. Similarly, a comparison of experimental and numerical TFs considering eight walking pedestrians is displayed in Fig. 17b. In both crowd scenarios, smooth curves are not longer obtained due to the presence of the pedestrians, but a good fit is observed between the experimental and numerical results in the frequency domain. Also, slight increments of the frequency of the crowd-structure systems can be guessed in comparison with the bare structure (Fig. 8b), and significant increments of the damping ratio are appreciated.

Since ζ_h is identified as the most relevant parameter of the model in the response prediction of the FRP footbridge (Section 5.3), values of 10%, 20%, and 30% are consider to observe the modification of G_{CL}. Fig. 18 displays the results for the weak and dense TCs. Based on the H_∞ norm in these graphs, adopting $\zeta_h = 10\%$ may over predict the structural response (in the safe side as shown in Fig. 15f), whilst $\zeta_h = 30\%$ may underestimate the bridge dynamic behaviour.

6.2. Pre-stressed concrete structure

The pre-stressed reinforced concrete footbridge built at the University of Sheffield is studied herein in terms of its TFs. Fig. 19a shows the simply supported structure, whose span, width and total weight are 10.8 m, 2 m, and 15 000 kg, respectively. The modal parameters of the first vertical vibration mode of the laboratory facility are: $m_{s1} = 6500$ kg [38], $f_{s1} = 4.44$ Hz, and $\zeta_{s1} = 0.72\%$ [36].

Numerical and experimental TFs are compared considering the derived $G_{CL}(s)$ (Eq. (32)) and the result of the test with six people (0.26 pedestrians/m^2) walking on the bridge reported by Živanović et al. [36]. To obtain the TF, the mass of the human body is

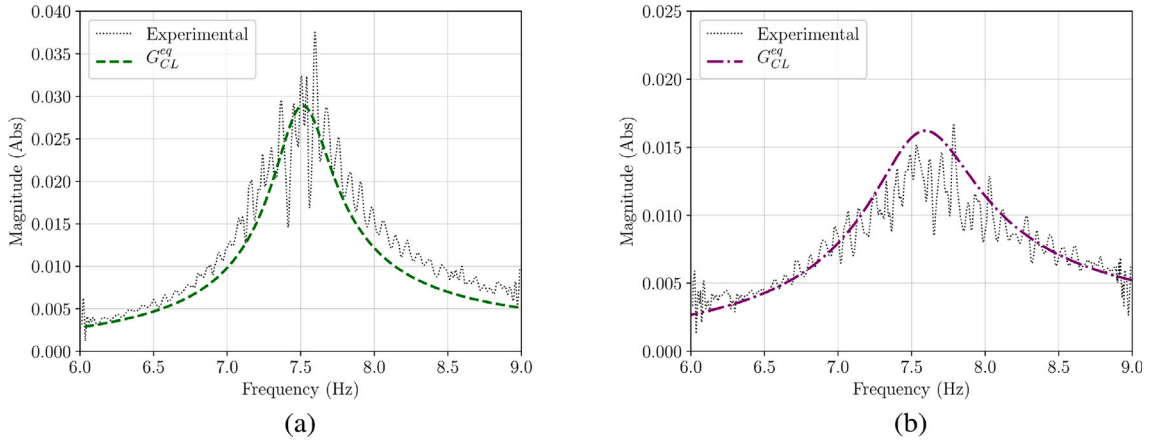

Fig. 17. Comparison of experimental and numerical TFs for the UPM footbridge: (a) Weak TC, and (b) Dense TC.

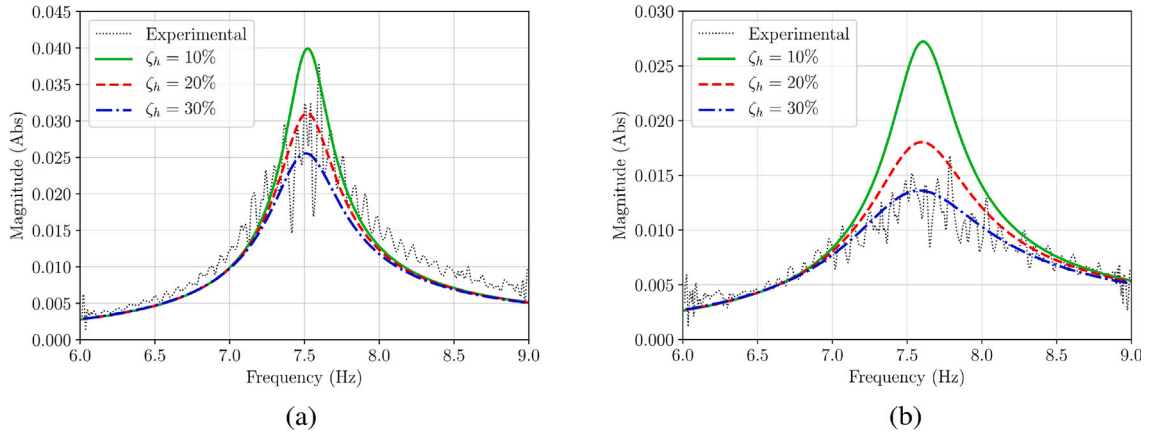

Fig. 18. Closed-loop TFs varying ζ_h of the UPM footbridge: (a) Weak TC, and (b) Dense TC.

$m_h = 0.93 \cdot 83$ kg, being 83 kg the mean value among the mass of the pedestrians involved in the experiment. Based on Refs. [39,40], the human body frequency is set equal to the gait frequency that causes resonant response ($f_h = f_a = f_s/r = 2.22$ Hz). Also, ζ_h take values of 10%, 20%, and 30%. Fig. 19b displays a comparison of experimental and numerical results, where a good match between the TFs is observed, especially for the case of $\zeta_h = 20\%$. This demonstrates that the proposed methodology leads to reasonable results even though the pedestrian-to-structure mass ratio for the experiment is 0.03.

7. Conclusions

A novel frequency-domain approach, which allows to predict the vertical response of a footbridge in a simple manner while considering HSI, has been proposed based on a coupled crowd-structure system. In this sense, a total closed-loop TF has been derived, and experimental and numerical results of two pedestrian structures have shown a good agreement employing the proposal. Considering the analyses carried out in this paper and the results obtained, the following conclusion may be drafted:

- In comparison with non-interacting pedestrian load models from existing guidelines, the proposed interacting approach allows an accurate computation of the MTVV of a simply supported FRP footbridge subjected to crowd actions.
- In contrast to previous works, the approach described in this paper presents no restrictions in terms of the pedestrian-to-structure mass ratio nor the structure natural frequencies.
- Since the proposed procedure is simpler to implement than time-domain approaches without loss of accuracy in the results, it may be suitable for reliability analyses while accounting for HSI.
- The use of the presented approach at the design stage of a lightweight footbridge may be practical for engineers given its simplicity and accuracy.
- The prediction of the response of a footbridge using the proposed interacting approach is more sensitive to the parameters of the human body, especially ζ_h, than the parameters of the structure.

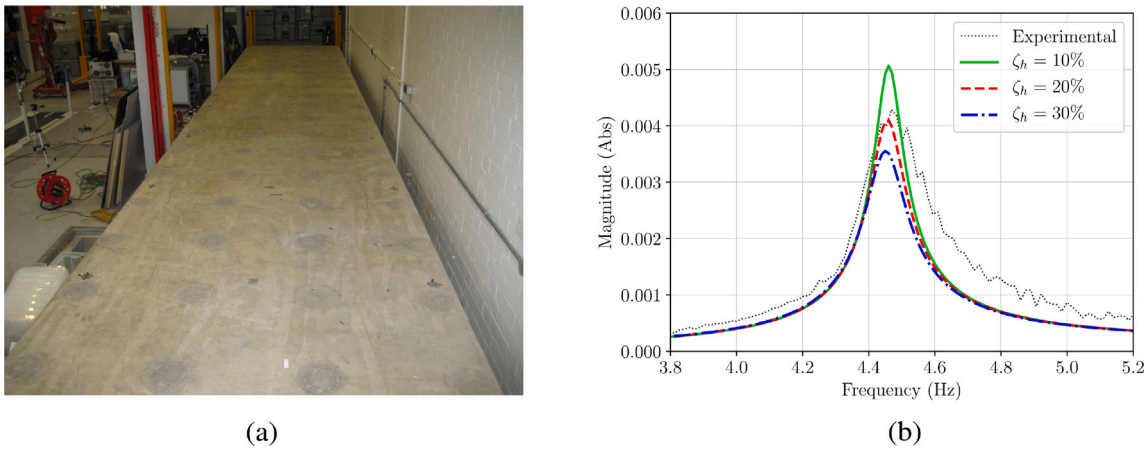

Fig. 19. Sheffield footbridge: (a) Structure, and (b) Closed-loop TFs varying ζ_h.

- The experimental and numerical TFs of coupled crowd-structure systems derived on two footbridges, an FRP bridge and a pre-stressed concrete structure, have shown good agreement. Thus, the proposed frequency-domain procedure is suitable for different pedestrian structures, regardless the material employed for their construction.
- Adopting lower values regarding the parameters of the human body may be preferable for a conservative evaluation of the response of a lightweight footbridge subjected to crowd loads. Values between 10% and 20% are recommended for ζ_h.

In the future, other type of lightweight structures considering different crowd scenarios will be studied to further validate the proposed framework. Also, synchronization among pedestrians will be investigated to determine if provisions established in existing guidelines can be directly applied to models that account for HSI. Accomplishing both tasks, a robust and easy-to-apply procedure to model CSI on footbridges could be proposed for inclusion in design guidelines.

CRediT authorship contribution statement

Christian Gallegos-Calderón: Conceptualization, Methodology, Software, Validation, Formal analysis, Investigation, Data curation, Writing – original draft, Visualization. **Javier Naranjo-Pérez:** Methodology, Software, Validation, Formal analysis, Investigation, Data curation, Writing – original draft, Visualization. **Carlos M.C. Renedo:** Methodology, Investigation, Writing – review & editing. **Iván M. Díaz:** Conceptualization, Methodology, Resources, Supervision, Writing – review & editing, Project administration, Funding acquisition.

Declaration of competing interest

The authors declare that they have no known competing financial interests or personal relationships that could have appeared to influence the work reported in this paper.

Data availability

Data will be made available on request.

Acknowledgements

The authors acknowledge the grant PID2021-127627OB-I00, funded by Ministerio de Ciencia e Innovación, Agencia Estatal de Investigación and 10.13039/501100011033 FEDER, European Union. Christian Gallegos-Calderón expresses his gratitude to Secretaría de Educación Superior, Ciencia, Tecnología e Innovación de Ecuador (SENESCYT) for the financial support. Javier Naranjo-Pérez thanks Ministerio de Universidades for the grant funded through the program 'European Union - NextGenerationEU'.

References

[1] R.A. Votsis, T.J. Stratford, M.K. Chryssanthopoulos, E.A. Tantele, Dynamic assessment of a FRP suspension footbridge through field testing and finite element modelling, Steel Compos. Struct. 23 (2017) 205–215.
[2] M. Gong, Y. Li, R. Shen, M. Asce, X. Wei, Glass suspension footbridge: Human-induced vibration, serviceability evaluation, and vibration mitigation, J. Bridge Eng. 26 (2021) 05021014.
[3] A. Tadeu, A. Romero, S. Dias, F. Pedro, M. Brett, M. Serra, P. Galvín, F. Bandeira, Vibration serviceability assessment of the world's longest suspended footbridge in 2020, Structures 44 (2022) 457–475.
[4] V. Boniface, V. Bui, P. Bressolette, P. Charles, X. Cespedes, Footbridges: Assessment of Vibrational Behaviour of Footbridges under Pedestrian Loading, Service d'Études Techniques des Routes et Autoroutes, Paris, 2006.
[5] C. Butz, C. Heinemeyer, A. Keil, M. Schlaich, A. Goldack, S. Trometer, M. Lukić, B. Chabrolin, A. Lemaire, P.-O. Martin, Á. Cunha, E. Caetano, HIVOSS: Design of footbridges guideline, Res. Fund. Coal Steel (2008).
[6] CEN, Draft PrEN 1990:2021 Basis of Structural and Geotechnical Design, Annex a.2. Applications for Bridges, European Committee for Standardisation, 2021.
[7] CEN, Draft PrEN 1991-2:2021: Actions on Structures — Part 2: Traffic Loads on Bridges and Other Civil Engineering Works, European Committee for Standardization, 2021.
[8] M. Bocian, J.M. Brownjohn, V. Racic, D. Hester, A. Quattrone, R. Monnickendam, A framework for experimental determination of localised vertical pedestrian forces on full-scale structures using wireless attitude and heading reference systems, J. Sound Vib. 376 (2016) 217–243.
[9] J. Chen, H. Tan, Z. Pan, Experimental validation of smartphones for measuring human-induced loads, Smart Struct. Syst. 18 (2016) 625–642.
[10] A. Firus, R. Kemmler, H. Berthold, S. Lorenzen, J. Schneider, A time domain method for reconstruction of pedestrian induced loads on vibrating structures, Mech. Syst. Signal Process. 171 (2022) 108887.
[11] P. Dey, S. Walbridge, S. Narasimhan, Vibration serviceability analysis of aluminum pedestrian bridges subjected to crowd loading, in: 6th International Conference on Advances in Experimental Structural Engineering, Urbana-Champaign, USA, 2015.
[12] E. Ahmadi, C. Caprani, S. Živanović, A. Heidarpour, Assessment of human-structure interaction on a lively lightweight GFRP footbridge, Eng. Struct. 199 (2019) 109687.
[13] E. Shahabpoor, A. Pavic, V. Racic, S. Zivanovic, Effect of group walking traffic on dynamic properties of pedestrian structures, J. Sound Vib. 387 (2017) 207–225.
[14] K. Van Nimmen, G. Lombaert, G. De Roeck, P. Van den Broeck, The impact of vertical human-structure interaction on the response of footbridges to pedestrian excitation, J. Sound Vib. 402 (2017) 104–121.
[15] I.M. Díaz, C.A. Gallegos-Calderón, J. Ramírez Senent, C.M.C. Renedo, Interaction phenomena to be accounted for human-induced vibration control of lightweight structures, Front. Built Environ. 7 (2021) 49.
[16] C.A. Jones, P. Reynolds, A. Pavic, Vibration serviceability of stadia structures subjected to dynamic crowd loads: A literature review, J. Sound Vib. 330 (2011) 1531–1566.
[17] E. Shahabpoor, A. Pavic, V. Racic, Interaction between walking humans and structures in vertical direction: A literature review, Shock Vib. 2016 (2016) 1–22.
[18] B. Lin, Q. Zhang, F. Fan, S. Shen, A damped bipedal inverted pendulum for human–structure interaction analysis, Appl. Math. Model. 87 (2020) 606–624.
[19] H. Yang, B. Wu, J. Li, Y. Bao, G. Xu, A spring-loaded inverted pendulum model for analysis of human-structure interaction on vibrating surfaces, J. Sound Vib. 522 (2022).
[20] J.F. Jiménez-Alonso, A. Sáez, E. Caetano, F. Magalhães, Vertical crowd-structure interaction model to analyze the change of the modal properties of a footbridge, J. Bridge Eng. 21 (2016).
[21] E. Shahabpoor, A. Pavic, V. Racic, Identification of mass–spring–damper model of walking humans, Structures 5 (2016) 233–246.
[22] F. Tubino, Probabilistic assessment of the dynamic interaction between multiple pedestrians and vertical vibrations of footbridges, J. Sound Vib. 417 (2018) 80–96.
[23] C. Gaspar, E. Caetano, C. Moutinho, J.G.S. da Silva, Active human-structure interaction during jumping on floors, Struct. Control Health Monit. 27 (2020) e2466.
[24] M.A. Toso, H.M. Gomes, F.T. Da Silva, R.L. Pimentel, Experimentally fitted biodynamic models for pedestrian-structure interaction in walking situations, Mech. Syst. Signal Process. 72–73 (2016) 590–606.
[25] C.M. Renedo, I.M. Díaz, J.M. Russell, S. Živanovic, Performance of inertial mass controllers for ultra-lightweight footbridges: A case study, in: Xi International Conference on Structural Dynamics EURODYN, Vol. 1, Athens, Greece, 2020, pp. 1741–1746.
[26] C. Gallegos-Calderón, J. Naranjo-Pérez, I.M. Díaz, J.M. Goicolea, Identification of a human-structure interaction model on an ultra-lightweight FRP footbridge, Appl. Sci. 11 (2021) 6654.
[27] E. Ahmadi, C.C. Caprani, A. Heidarpour, An equivalent moving force model for consideration of human-structure interaction, Appl. Math. Model. 51 (2017) 526–545.
[28] K. Van Nimmen, A. Pavic, P. Van den Broeck, A simplified method to account for vertical human-structure interaction, Structures 32 (2021) 2004–2019.
[29] ISO, ISO 10137 - Bases for Design of Structures - Serviceability of Buildings and Walkways Against Vibrations, Vol. 10137, International Organization for Standardization, 2007.
[30] Fiberline Composites A/S, General Design Certification Fiberline Composites A/S, Middelfart, Denmark, 2018.
[31] C. Gallegos-Calderón, J. Naranjo-Pérez, M.D.G. Pulido, I.M. Díaz, Design, construction and structural response of a lightweight FRP footbridge, in: IABSE Congress: Structural Engineering for Future Societal Needs, Ghent, 2021, pp. 2053–2061.
[32] PCB-Piezotronics, Accelerometer Model 393A03, PCB Piezotronics Inc, 2018.
[33] APS, APS 400 ELECTRO-SEIS® - Long Stroke Shaker with Linear Ball Bearings, APS Dynamics Inc., 2013.
[34] SIMULIA, Abaqus 2020 Analysis User's Guide, Dassault Systèmes Simulia Corporation, 2020.
[35] M. Alqam, R.M. Bennett, A.H. Zureick, Three-parameter vs. two-parameter Weibull distribution for pultruded composite material properties, Compos. Struct. 58 (2002) 497–503.
[36] S. Živanović, I. Díaz, A. Pavić, Influence of walking and standing crowds on structural dynamic properties, in: IMAC XXVII Conference & Exposition on Structural Dynamics, The Society for Experimental Mechanics, Inc., Orlando, FL, 2009.
[37] K. Ogata, Modern Control Engineering, fifth ed., Prentice Hall, 2010.
[38] S. Živanović, G. Feltrin, J.T. Mottram, J.M. Brownjohn, Vibration performance of bridges made of fibre reinforced polymer, in: Conference Proceedings of the Society for Experimental Mechanics Series, Vol. 4, Orlando, FL, 2014, pp. 155–162.
[39] E. Ahmadi, C. Caprani, S. Živanović, A. Heidarpour, Experimental validation of moving spring-mass-damper model for human-structure interaction in the presence of vertical vibration, Structures 29 (2021) 1274–1285.
[40] M. Zhang, C.T. Georgakis, J. Chen, Biomechanically excited SMD model of a walking pedestrian, J. Bridge Eng. 21 (2016) C4016003.